Hindawi
International Journal of Antennas and Propagation
Volume 2017, Article ID 5375036, 8 pages
https://doi.org/10.1155/2017/5375036

Research Article

Suppressed Band Characteristics of an UWB Conical Monopole Antenna with Split Loops Based on the Equivalent Circuit

Eun-Seok Jang,[1] Che-Young Kim,[1] Dae-Geun Yang,[1] and Sung-Su Hong[1,2]

[1]*School of Electronics Engineering, Kyungpook National University, 80 Daehakro, Buk-gu, Daegu 41566, Republic of Korea*
[2]*Department of Equipment Applied Research, Gyeongbuk Research Institute of Vehicle Embedded Technology, 97-70 Myeongsan-gil, Yeongcheon, Gyeongsangbuk-do 38822, Republic of Korea*

Correspondence should be addressed to Che-Young Kim; cykim@ee.knu.ac.kr

Received 7 October 2016; Revised 2 January 2017; Accepted 22 January 2017; Published 12 February 2017

Academic Editor: Toni Björninen

In this study, the principle of band suppressing an UWB antenna by attaching a small resonator is explained by developing its equivalent circuit. The realized UWB antenna is a conical monopole antenna that contains a split loop for band suppression. The conical monopole antenna corresponds to a transmission line terminated with load impedance, and the split loop is an LC resonator. The coupling between the conical monopole antenna and the split loop is represented as mutual inductance. Equivalent circuits for the UWB antenna suppressing single band [WLAN] and dual band [WLAN, WiMAX] have been suggested, and these equivalent circuits provide insight into the performance characteristics of the developed band suppressed UWB antenna to which a small sized resonator is installed. Simulation and measurement results on the input impedance and VSWR of the proposed equivalent circuit are closely matched. Thus, the validity of the equivalent circuit is confirmed. The measurement results demonstrate that the proposed antenna exhibits a gain of over 3 dBi in the working band and has an omnidirectional radiation pattern. Band rejection has been also implemented by split loops.

1. Introduction

Since 2002, the FCC has permitted the commercial use of the 3.1 GHz~10.6 GHz band to meet the need of high capacity communication at short ranges. Since then, research on developing antennas for UWB wireless communication systems began in earnest. Mainly, the planar type antennas have been developed [1–6], and a few three-dimensional antennas have been reported [7–11]. Interference occurs in UWB systems because other communication bands coexist within this frequency range. In order to solve this problem, band-notched UWB antennas that contain a stub or a small resonator have been reported [12–21].

Equivalent circuits that describe the performance characteristic of band rejection UWB antennas have been also reported [22–26]. The equivalent circuit models were derived from macro model and vector fitting [22, 23]. However, the equivalent circuits of these two studies are not appropriate for explaining operational characteristic of antennas, because they lack consideration on the electromagnetic property of antennas structures. Although overall figure of equivalent circuit was derived for the antenna structure, the way of treatment was similar to category of the above two studies [24]. There are studies that report the equivalent circuit derived from electromagnetic property of antennas structure. But impedance result of the equivalent circuit is not close to simulation result or they show about 30% rejection band difference between equivalent circuit and simulation result [25, 26]. In our study, the equivalent circuit of band suppressed UWB antenna is rooted on electromagnetic property of antennas structure, and also VSWR of the equivalent circuit matches with simulation within 10%. Although the equivalent circuit composed of a planar type transmission line and split ring resonators has been reported [27], research specifically regarding equivalent circuits of UWB antennas which include small resonators has been scant.

In this paper, several equivalent circuits of band rejection UWB antennas that include small resonators are investigated

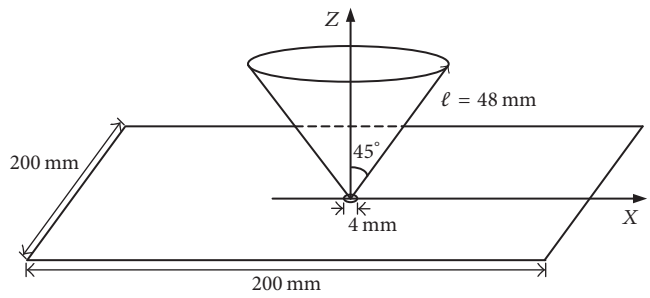

Figure 1: Geometry and dimensions of primitive UWB antenna.

and the physical reasoning of each assigned element value is provided. The equivalent circuits are realized for the conical monopole antenna with split loops. The conical monopole antenna is representative of wide band antennas and can be implemented for UWB by adjusting the length and angle of the cone. The split loop is an open shaped resonator whose resonant frequency is controlled by adjusting the diameter of the loop. In this study, a split loop that resonates at WLAN (5.8 GHz) and a split loop that resonates at WiMAX (3.5 GHz) were attached to UWB antenna. A single band [WLAN (5.8 GHz)] suppressed UWB antenna and dual band [WLAN (5.8 GHz), WiMAX (3.5 GHz)] suppressed UWB antenna were realized and their equivalent circuits for these antennas were proposed. The equivalent circuits were validated by comparing their input impedance and VSWR with the realized antennas, which implemented bands notched at WiMAX and WLAN and exhibited an omnidirectional radiation pattern and a measured gain of over 3 dBi.

2. Conical Monopole UWB Antenna

The geometry and dimensions of the conical monopole antenna for UWB are depicted in Figure 1.

The structure shown in Figure 1 is modeled as a spherical coaxial transmission line, and the characteristic resistance is obtained from (1) [28]. The angle of the cone is set to 45° to give 50 Ω.

$$Z_0 = 60 \ln\left(\cot\frac{\theta}{2}\right). \tag{1}$$

The length of the cone has to be decided after the angle of the cone is established. As the length of the conical monopole antenna increases, the input impedance converges to the characteristic impedance of a spherical coaxial transmission line. Obviously, the length of the cone cannot increase to infinity. Thus, a proper length should be selected and its value can be determined through (2a), (2b), and (2c) [29], where k is the wave number and ℓ is the length of the conical monopole antenna.

$$Z_{\text{in}} = Z_0 \frac{1-\Delta}{1+\Delta}, \tag{2a}$$

where

$$\Delta = e^{-2jk\ell} \frac{1 + j\left(60/Z_0\right) \sum_{n=1}^{\infty} \left((2n+1)/n(n+1)\right) \left[P_n(\cos\theta)\right]^2 \zeta_n(k\ell)}{-1 + j\left(60/Z_0\right) \sum_{n=1}^{\infty} \left((2n+1)/n(n+1)\right) \left[P_n(\cos\theta)\right]^2 \zeta_n(k\ell)} \tag{2b}$$

$$\zeta_n(k\ell) = \frac{h_n^{(2)}(k\ell)}{h_{n-1}^{(2)}(k\ell) - (n/k\ell)\, h_n^{(2)}(k\ell)}. \tag{2c}$$

P_n in (2a), (2b), and (2c) is the nth-order Legendre function and $h_n^{(2)}$ in (2a), (2b), and (2c) is a second-kind Hankel function. Figure 2 has been derived by calculating (2a), (2b), and (2c). From Figure 2, if $k\ell$ is between 2 and 4, then the impedance lies between 40 Ω and 60 Ω. The impedance in this range results in a VSWR of 2 or below across the frequency range 3.1 GHz to 10.6 GHz. Taking into account the above guideline and antenna trimming, the length of the antenna is decided to be slightly longer than 40 mm up to 48 mm. The influence of the antenna ground size has been explained in our preceding research work [18].

3. Split Loop

When the split loop resonates, its impedance changes rapidly. Thus, the input impedance of the antenna with the split loop varies drastically. At this moment, a mismatch occurs between the antenna body and the feeding part. Because of this mismatch, the antenna has a band rejection characteristic if the split loop is attached to the antenna. The geometry and the equivalent circuit of the split loop are shown in Figure 3.

The equivalent circuit of the split loop is an LC resonant circuit. Inductance and capacitance of the LC resonator are calculated from (3) and (4), respectively [30]. Equation (4) is

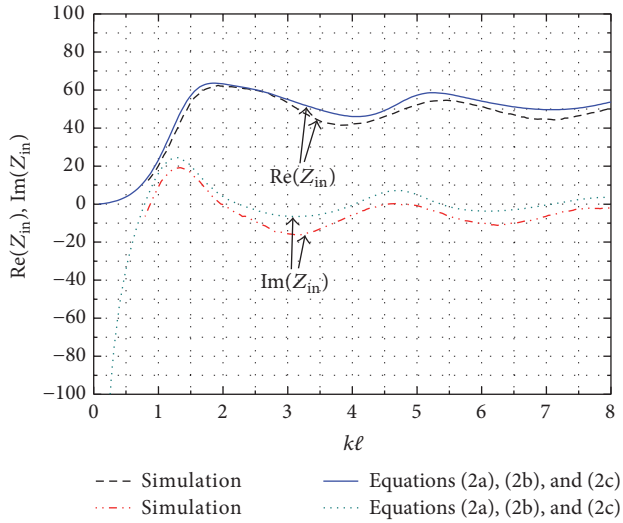

Figure 2: Input impedance of a conical type monopole antenna.

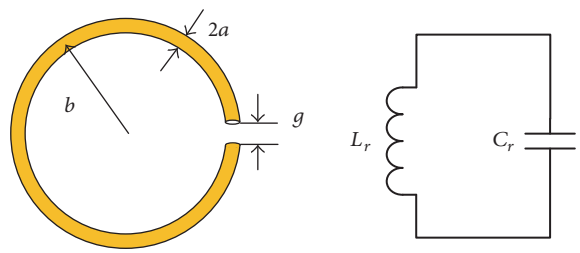

Figure 3: Geometry of a split loop and its equivalent circuit.

the sum of loop capacitance and of gap capacitance loaded to the loop.

$$L_r = \mu_0 b \ln \frac{b}{a}, \tag{3}$$

$$C_r = \frac{1}{3} \frac{\epsilon_0 \pi^2 b}{\ln (b/a)} + \frac{\epsilon_0 \pi a^2}{g}. \tag{4}$$

The resonant frequency of the split loop is determined from $f_r = 1/(2\pi\sqrt{L_r C_r})$. The dimensions of a split loop for resonance value of 3.5 GHz and 5.8 GHz resonance are found from (3), (4), and the resonant frequency formula. The determined dimensions are listed in Table 1.

The resonant frequency of the split loop is controlled by adjusting its radius b. Two values of b for each frequency are written in Table 1. Upper values are calculated from (3) and (4). Lower values are dimensions that were optimized through simulating the antenna with the split loop. Little difference is observed between the upper values and the lower values. Thus, (3) and (4) can be used admittedly for deciding the initial dimensions before the split loops are installed to the antenna. In addition, the proposed equivalent circuit of the split loop can be applied to the equivalent model of a band-notched UWB antenna because the difference is not large between the operating frequencies before and after the split loop is mounted on the antenna.

Table 1: Dimension of split loop.

Frequency	b (loop radius)	a (wire radius)	g (gap)
3.5 GHz	6.5 mm (calculated) 5.8 mm (simulated)	0.5 mm	0.3 mm
5.8 GHz	3.8 mm (calculated) 3.5 mm (simulated)	0.5 mm	0.3 mm

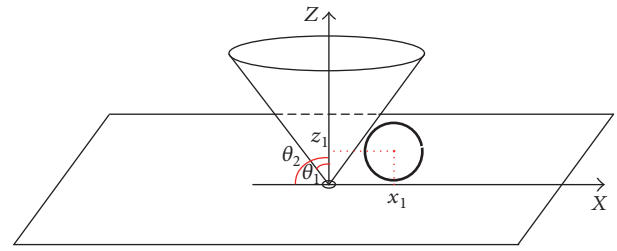

Figure 4: Geometry of a cone type monopole UWB antenna with a split loop.

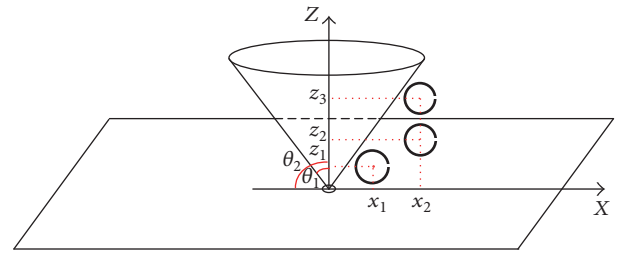

Figure 5: Position variation of the 5.8 GHz split loop ($x_1 = 10$ mm, $x_2 = 20$ mm, $z_1 = 4.2$ mm, $z_2 = 10$ mm, and $z_3 = 14$ mm).

4. Bands Suppressed UWB Antenna

4.1. Single Band Suppressed UWB Antenna. A conical monopole UWB antenna, combined with a split loop, is described in Figure 4. The dimensions of the conical monopole antenna are identical to the dimensions of Figure 1.

In order to decide the position of the split loop, we exploit the VSWR variation by moving the split loop position at 5.8 GHz as illustrated in Figure 5. When the position is near the feeding point, the antenna has on-band rejection characteristic. On the other hand, when the position is far from the feeding point, the antenna has out-of-band rejection characteristic. These features are shown in Figure 6. This characteristic is from the fact that the magnetic intensity would be strong near around the feeding point. Hence, the split loop should be put near the feeding point as indicated by $x_1 = 10$ mm and $z_1 = 4.2$ mm in Figure 5. And this configuration brings the magnetic field passed through the area of loop perpendicularly.

Based on Figures 5 and 6, we used a 3.5 mm radius split loop to obtain a single 5.8 GHz band suppressed characteristic as seen in Figure 4.

Figure 7 is the equivalent circuit of the antenna shown in Figure 4. The transmission line in Figure 7 corresponds to the conical monopole antenna. Because the magnetic field of the antenna passes through the split loop, mutual inductance

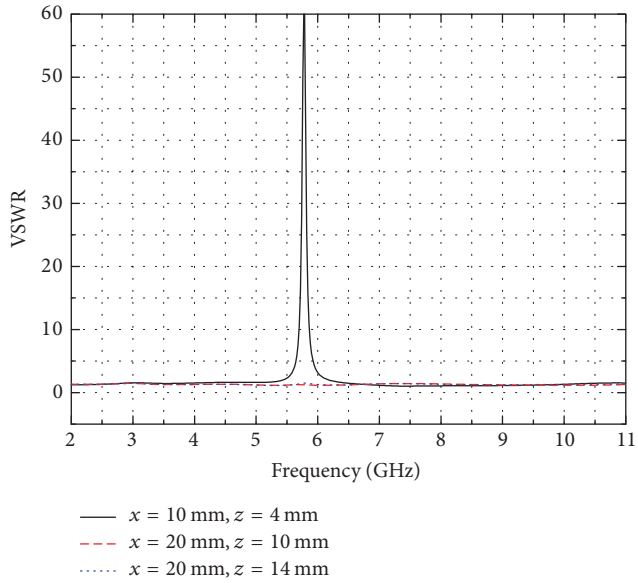

Figure 6: Comparison of simulated VSWR results depending on positions of the split loop.

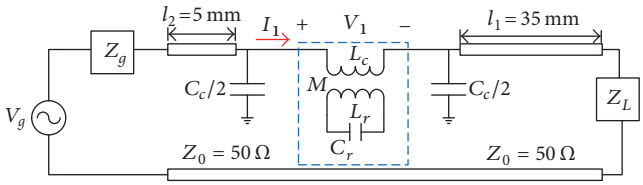

Figure 7: Equivalent circuit of a band suppressed cone type monopole UWB antenna.

exists between the two components. The transformer in the middle of Figure 7 represents the combination of the conical monopole antenna and the split loop. The load impedance connected to the end of the transmission line is obtained from the following equation, which is a retroactive formula about the input impedance of the conical monopole antenna:

$$Z_L = Z_0 \frac{Z_{\text{in}} - jZ_0 \tan \beta l}{Z_0 - jZ_{\text{in}} \tan \beta l}. \tag{5}$$

In order to derive the impedance of the transformer, reflected impedance is adopted. Thus, Figure 8 corresponds to Figure 7, where Z_{R1} in Figure 8 is the reflected impedance of the transformer of Figure 7. Equations (6a) and (6b) are the interaction formula for the reflected impedance and the elements which constitute the transformer.

$$Z_{R1} = \frac{j\omega^3 M^2 C_r}{1 - (\omega/\omega_0)^2}, \tag{6a}$$

where

$$\omega_0 = \frac{1}{\sqrt{L_r C_r}}. \tag{6b}$$

In (6b), ω_0 is a resonance angular frequency of the split loop. The values of L_r, C_r, L_c, C_c, and M need to be obtained before the input impedance of the equivalent circuit in Figure 8 is calculated. M that appeared in (6a) and (7) represents the mutual inductance between the conical monopole antenna and the split loop. Equation (7) has been derived by integrating the magnetic field passed through the split loop. In order to obtain (8) and (9), the range occupied by the split loop in the antenna has been considered.

$$M = \int_0^{2\pi} \int_0^b \frac{\mu_0 r \, dr \, d\theta}{2\pi \sqrt{(r \sin\theta - x_1)^2 + (r \cos\theta - z_1)^2} \sin\left(\tan^{-1}\left((r \sin\theta - z_1)/(r \cos\theta - x_1)\right)\right)}, \tag{7}$$

$$L_c = \frac{\mu_0 b}{\pi} \ln \left| \tan \frac{\theta_2}{2} \cot \frac{\theta_1}{2} \right|, \tag{8}$$

$$C_c = \frac{4\pi\epsilon_0 b}{\ln\left(\tan\left((\theta_2 - \theta_1)/2\right)\right)}. \tag{9}$$

In here, L_c and C_c are the inductance and the capacitance of the antenna, respectively. The dimensions for the 5.8 GHz split loop in Table 1 are used to calculate the element values. The calculated element values from (3), (4), (7), (8), and (9) are summarized in Table 2. These values have been used to calculate the input impedance and the VSWR of the equivalent circuit in Figure 8.

The input impedance and VSWR results of the simulation and the equivalent circuit are plotted in Figure 9. The results of the equivalent circuit are closely matched to those of simulation. In particular, the center frequency 5.8 GHz of the suppressed band in Figure 9(b) is identical to the resonant frequency $1/(2\pi\sqrt{L_r C_r})$ of the split loop. Thus, the proposed equivalent circuit is quite good for analyzing the split loop mounted antenna.

4.2. Double Bands Suppressed Antenna. The antenna with two split loops, which suppress the 3.5 GHz band and the 5.8 GHz band, is shown in Figure 10. The left side split loop is for 3.5 GHz band rejection and the right side split loop is for 5.8 GHz band rejection.

The equivalent circuit of dual band suppressed UWB in Figure 10 is exhibited in Figure 11. The reflected impedance

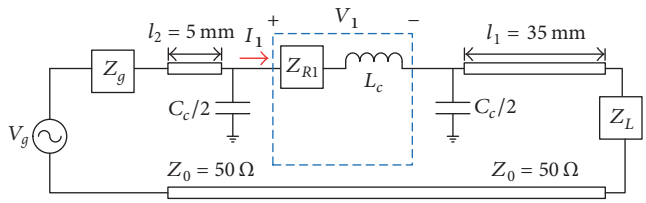

Figure 8: Simplified equivalent circuit of a band suppressed cone type monopole UWB antenna.

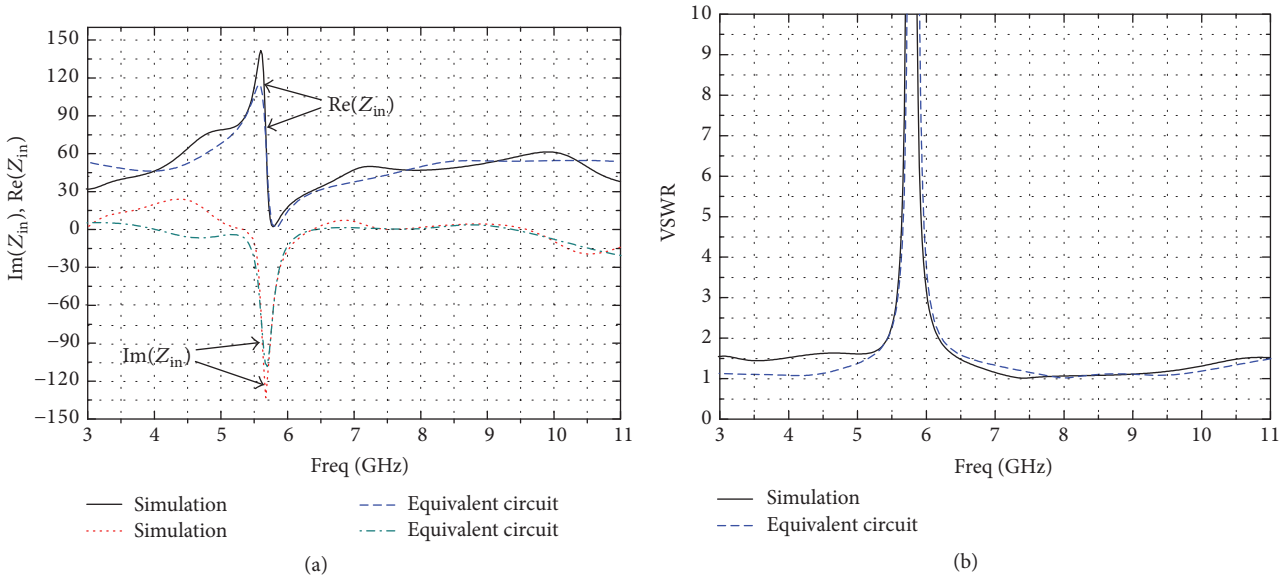

Figure 9: Comparison of simulated and calculated result for the equivalent circuit (a) input impedance and (b) VSWR.

Table 2: Calculated result of elements for equivalent circuit in Figure 8.

Split loop	L_r	C_r	M	L_c	C_c
5.8 GHz	9.68 nH	0.077 pF	1.01 nH	1.1 nH	4.4 pF

Table 3: Calculated result of elements for the equivalent circuit in Figure 11.

Split loop	L_r	C_r	M	L_c	C_c
3.5 GHz	20.09 nH	0.097 pF	1.77 nH	1.2 nH	4.7 pF
5.8 GHz	9.68 nH	0.077 pF	1.01 nH	1.2 nH	4.7 pF

Z_{R2} responsible for the left side loop appeared in series with Z_{R1} in Figure 8 to obtain equivalent circuit for Figure 10.

The two split loops are placed symmetrically at the same positions as seen in Figure 10. Each split loop shares the inductor of the conical antenna with the other split loop. This condition can be construed as series connection of the two reflected impedances. The reflected impedance Z_{R1} and impedance Z_{R2} in Figure 11 are for the 5.8 GHz and 3.8 GHz split loop, respectively.

The dimensions of the 3.5 GHz and 5.8 GHz split loops in Table 1 were entered into the equations of the elements, and then each element value was calculated. The results of calculation are tabulated in Table 3. The input impedance and VSWR of the equivalent circuit in Figure 11 are obtained from the values in Table 3. The values of L_c and C_c have been optimized between the radius of the 5.8 GHz split loop and that of the 3.5 GHz split loop.

To investigate the rotational angle effect between two loops, 3.5 GHz split loop was rotated 10° with respect to the fixed 5.8 GHz loop like Figure 12. The contours in Figure 13 show comparisons of VSWR for Figures 10 and 12. We observe that VSWR does not change even when one loop is rotated about the reference loop. Therefore, any angle placement between 3.5 GHz loop and 5.8 GHz loop is acceptable as far as the split loops are located near the feeding point.

The fabricated antenna is shown in Figure 14. The inverted triangle in the structure is the conical antenna. The plane at the bottom is the ground of the antenna. The coaxial feeding part locates between the apex of the conical monopole antenna and the ground plane. The two split loops of different radii are attached to expanded polystyrene whose dielectric constant is almost unity.

VSWR results of simulation, measurements, and the equivalent circuit are similar to each other as shown in Figure 15. The center frequencies 3.5 GHz and 5.8 GHz of each suppressed band in Figure 15 are identical to resonance frequencies $1/(2\pi\sqrt{L_rC_r})$ of the two split loops that vary in

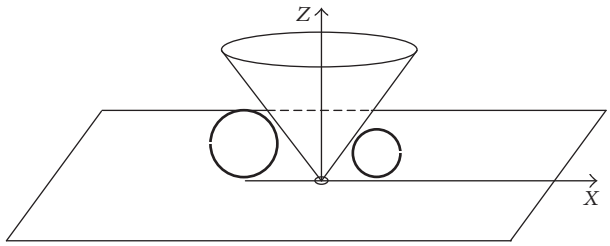

Figure 10: Geometry of a conical monopole UWB antenna with two split loops.

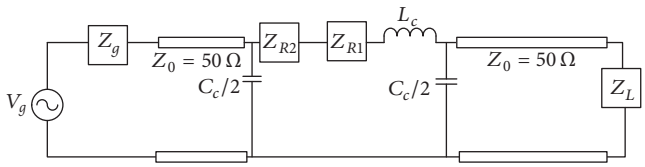

Figure 11: Equivalent circuit of two bands suppressed conical monopole UWB antenna.

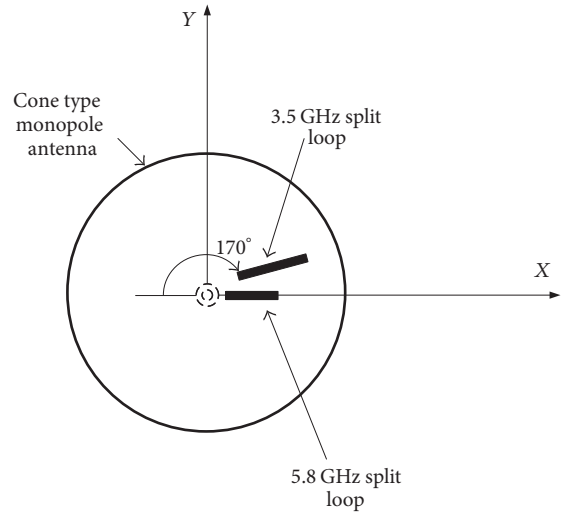

Figure 12: Top view of the antenna when 3.5 GHz split loop is rotated.

radius. This suggests that the equivalent circuit of the dual band-notched UWB antenna indeed describes the rejection characteristic of an UWB antenna, which includes two small resonators with different resonant frequencies.

5. Antenna Gain and Radiation Pattern

The antenna gain and radiation pattern of the proposed antenna are shown in Figures 16 and 17, respectively [18]. In here, two nulls at 3.5 GHz and 5.8 GHz are observed as band suppression, as expected.

The antenna gain is over 3 dBi in the working band and the dropped gain at the target rejection bands of 3.5 GHz and 5.8 GHz is observed in Figure 16. The radiation patterns in Figure 17 are omnidirectional and show a 5 dBi antenna gain at 4.5 GHz. Based on the presented figures, we know that the realized antenna properly functions as a band rejected UWB antenna.

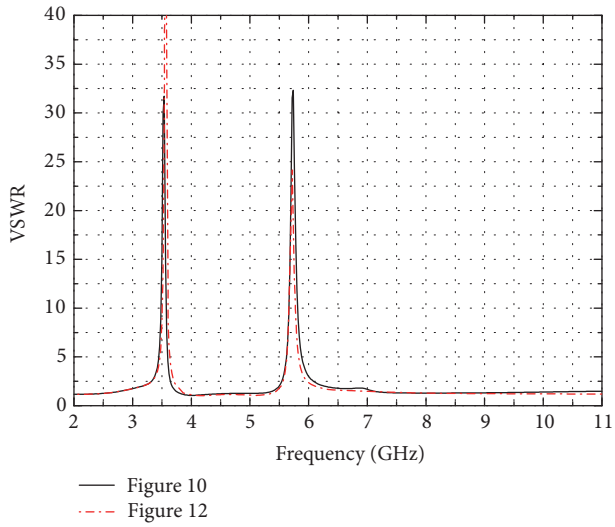

Figure 13: Simulated VSWR of Figures 10 and 12.

6. Conclusion

In this paper, a conical monopole antenna installed with split loops was designed to work as a band suppressed UWB antenna. The equivalent circuit for the designed antenna was proposed to describe the performance characteristic of a band rejected UWB antenna that includes small resonators. The equivalent model of the realized antenna is a circuit composed of a transmission line and a transformer. The transmission line corresponds to the conical monopole antenna and the transformer models the coupling between the LC resonator and the implicit inductance of the conical monopole antenna. The equivalent circuits for the UWB antenna notching single band (5.8 GHz) and dual band (3.5 GHz, 5.8 GHz) were derived, respectively. The input impedance and VSWR of the equivalent circuits agreed with the results of simulation and measurement. In particular, the suppressed bands of the

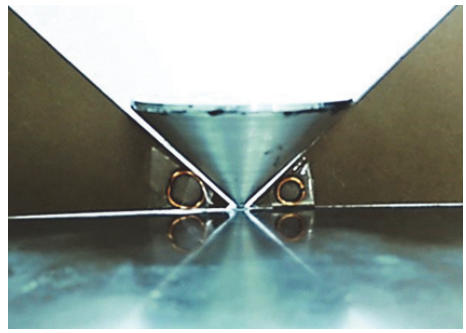

Figure 14: Fabricated dual band suppressed conical monopole UWB antenna.

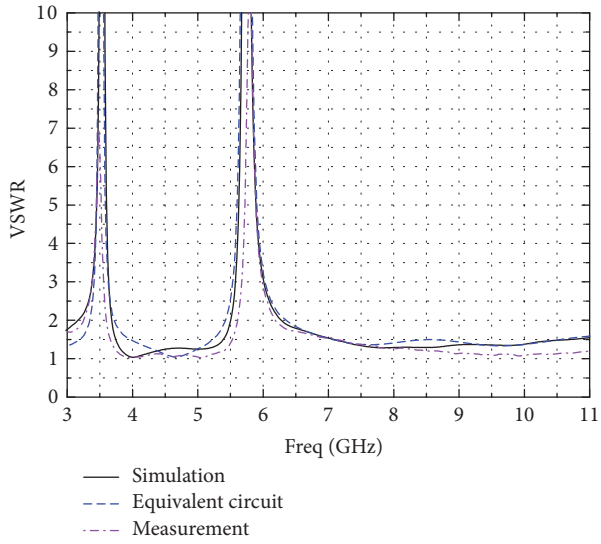

Figure 15: Comparison of simulated and measured VSWR for antenna structure and calculated VSWR for the equivalent circuit.

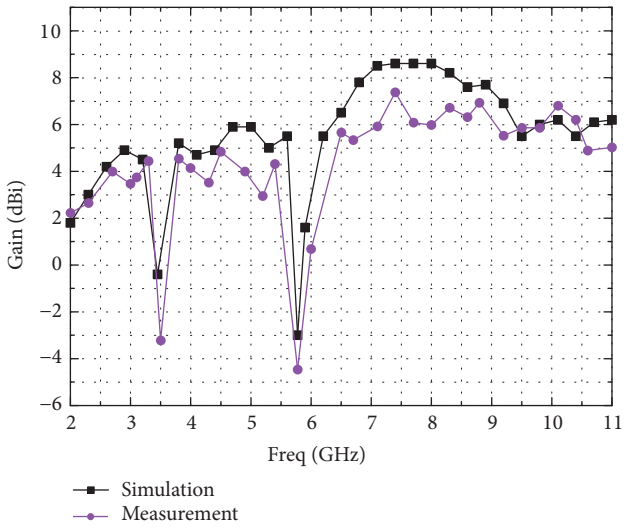

Figure 16: Simulated and measured gain of the antenna.

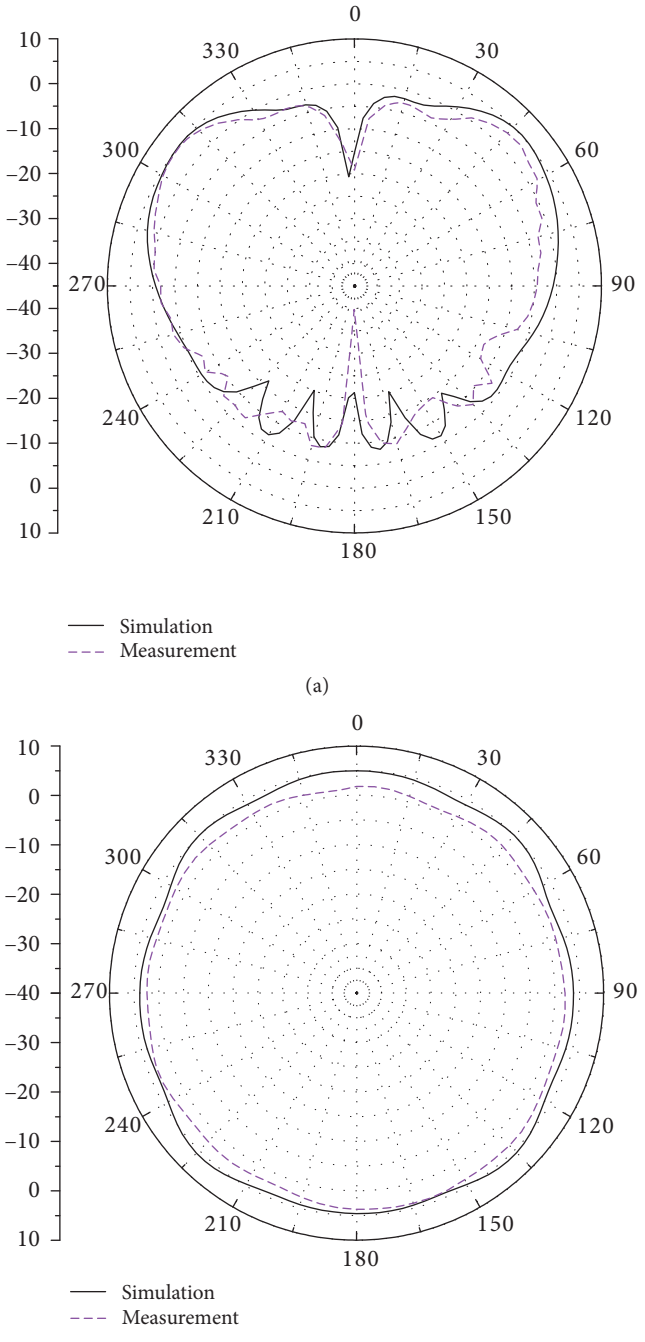

Figure 17: Comparison of simulated radiation patterns and measured radiation patterns at 4.5 GHz: (a) E-plane and (b) H-plane.

equivalent circuits are identical with the results of simulation and measurement. The realized dual band suppressed UWB antenna shows the omnidirectional characteristic and over 3 dBi antenna gain at frequencies where rejection does not occur. The suggested equivalent circuits provide physical insight into the operational mechanism of band suppressed UWB antennas and also help to bridge the gap between the physical antenna structure and its performance.

Competing Interests

The authors declare that there is no conflict of interests regarding the publication of this paper.

Acknowledgments

This study was supported by BK21 Plus Project funded by the Ministry of Education, Korea (21A20131600011).

References

[1] D. Chen and C. H. Cheng, "A novel compact ultra-wideband (UWB) wide slot antenna with via holes," *Progress in Electromagnetics Research*, vol. 94, pp. 343–349, 2009.

[2] J. R. Verbiest and G. A. E. Vandenbosch, "A novel small-size printed tapered monopole antenna for UWB WBAN," *IEEE Antennas and Wireless Propagation Letters*, vol. 5, no. 1, pp. 377–379, 2006.

[3] J. Liu, S. Gong, Y. Xu, X. Zhang, C. Feng, and N. Qi, "Compact printed ultra-wideband monopole antenna with dual band-notched characteristics," *Electronics Letters*, vol. 44, no. 12, pp. 710–711, 2008.

[4] Y.-J. Ren and K. Chang, "An annual ring antenna for UWB communications," *IEEE Antennas and Wireless Propagation Letters*, vol. 5, no. 1, pp. 274–276, 2006.

[5] D.-O. Kim and C.-Y. Kim, "CPW-fed ultra-wideband antenna with triple-band notch function," *Electronics Letters*, vol. 46, no. 18, pp. 1246–1248, 2010.

[6] L. A. Yimdjo Poffelie, P. J. Soh, S. Yan, and G. A. Vandenbosch, "A high-fidelity all-textile UWB antenna with low back radiation for off-body WBAN applications," *IEEE Transactions on Antennas and Propagation*, vol. 64, no. 2, pp. 757–760, 2016.

[7] Z. H. Hu, P. S. Hall, J. R. Kelly, and P. Gardner, "Improved band-notched wideband conical monopole antenna," *Microwave and Optical Technology Letters*, vol. 53, no. 8, pp. 1825–1829, 2011.

[8] S. Soheily, A. A. Dastranj, M. Mahzoon et al., "Design and optimization of a cone shaped monopole antenna," *Journal of Basic and Applied Scientific Research*, vol. 3, pp. 375–380, 2013.

[9] S. Palud, F. Colombel, M. Himdi, and C. Le Meins, "A novel broadband eighth-wave conical antenna," *IEEE Transactions on Antennas and Propagation*, vol. 56, no. 7, pp. 2112–2116, 2008.

[10] T. S. P. See and Z. N. Chen, "An electromagnetically coupled UWB plate antenna," *IEEE Transactions on Antennas and Propagation*, vol. 56, no. 5, pp. 1476–1479, 2008.

[11] H. Zhou, Q. Liu, B. Sun, and Y. Yang, "A band-notched swallow-tailed planar monopole antenna for UWB application," *Microwave and Optical Technology Letters*, vol. 50, no. 3, pp. 793–795, 2008.

[12] R. Fallahi, A.-A. Kalteh, and M. G. Roozbahani, "A novel UWB elliptical slot antenna with band-notched characteristics," *Progress in Electromagnetics Research*, vol. 82, pp. 127–136, 2008.

[13] S. Jacob, A. O. Lindo, C. M. Nijas, C. K. Aanandan, and P. Mohanan, "Analysis of CPW-Fed UWB antenna for WIMAX and WLAN band rejection," *Progress In Electromagnetics Research C*, vol. 52, pp. 83–92, 2014.

[14] D. Sarkar, K. V. Srivastava, and K. Saurav, "A compact microstrip-fed triple band-notched UWB monopole antenna," *IEEE Antennas and Wireless Propagation Letters*, vol. 13, pp. 396–399, 2014.

[15] T. Li, H. Zhai, G. Li, L. Li, and C. Liang, "Compact UWB band-notched antenna design using interdigital capacitance loading loop resonator," *IEEE Antennas and Wireless Propagation Letters*, vol. 11, pp. 724–727, 2012.

[16] D.-O. Kim, N.-I. Jo, D.-M. Choi, and C.-Y. Kim, "Design of the ultra-wideband antenna with 5.2 GHz/5.8 GHz band rejection using rectangular split-ring resonators (SRRS) loading," *Journal of Electromagnetic Waves and Applications*, vol. 23, no. 17-18, pp. 2503–2512, 2009.

[17] Y. Sung, "UWB monopole antenna with two notched bands based on the folded stepped impedance resonator," *IEEE Antennas and Wireless Propagation Letters*, vol. 11, pp. 500–502, 2012.

[18] D.-O. Kim, N.-I. Jo, H.-A. Jang, and C.-Y. Kim, "Design of the ultrawideband antenna with a quadruple-band rejection characteristics using a combination of the complementary split ring resonators," *Progress in Electromagnetics Research*, vol. 112, pp. 93–107, 2011.

[19] E. S. Jang, K. Kim, J. K. Park, and C.-Y. Kim, "A selective robust SRR providing notched band in conical monopole UWB antenna," *Microwave and Optical Technology Letters*, vol. 58, no. 2, pp. 332–337, 2016.

[20] H. Peng, C. Wang, L. Zhao, and J. Liu, "Novel SRR-loaded CPW-fed UWB antenna with wide band-notched characteristics," *International Journal of Microwave and Wireless Technologies*, 2016.

[21] J. Acharjee, K. Mandal, S. K. Mandal, and P. P. Sarkar, "A compact printed monopole antenna with enhanced bandwidth and variable dual band notch for UWB applications," *Journal of Electromagnetic Waves and Applications*, vol. 30, no. 15, pp. 1980–1992, 2016.

[22] Y. Wang, J. Z. Li, and L. X. Ran, "An equivalent circuit modeling method for ultra-wideband antennas," *Progress in Electromagnetics Research*, vol. 82, pp. 433–445, 2008.

[23] M. M. M. Ali, A. A. R. Saad, and E. E. M. Khaled, "A microstrip-fed printed slot antenna for 3G/Bluetooth/WiMAX and UWB applications with 3.6GHz Band rejection," in *Proceedings of the Progress in Electromagnetics Research Symposium (PIERS '13)*, pp. 588–592, Stockholm, Sweden, August 2013.

[24] F. Zhu, S. Gao, A. T. S. Ho et al., "Multiple band-notched UWB antenna with band-rejected elements integrated in the feed line," *IEEE Transactions on Antennas and Propagation*, vol. 61, no. 8, pp. 3952–3960, 2013.

[25] T.-G. Ma and S.-J. Wu, "Ultrawideband band-notched folded strip monopole antenna," *IEEE Transactions on Antennas and Propagation*, vol. 55, no. 9, pp. 2473–2479, 2007.

[26] Q.-X. Chu and Y.-Y. Yang, "A compact ultrawideband antenna with 3.4/5.5 GHz dual band-notched characteristics," *IEEE Transactions on Antennas and Propagation*, vol. 56, no. 12, pp. 3637–3644, 2008.

[27] J. D. Baena, J. Bonache, F. Martín et al., "Equivalent-circuit models for split-ring resonators and complementary split-ring resonators coupled to planar transmission lines," *IEEE Transactions on Microwave Theory and Techniques*, vol. 53, no. 4, pp. 1451–1461, 2005.

[28] J. D. Kraus, "The biconical antenna and its impedance," in *Antennas*, chapter 8, p. 347, McGraw Hill, Boston, Mass, USA, 2nd edition, 1988.

[29] C. H. Papas and R. King, "Input impedance of wide-angle conical antennas fed by a coaxial line," *Proceedings of the IRE*, vol. 37, no. 11, pp. 1269–1271, 1949.

[30] S. A. Schelkunoff and H. T. Friis, "Small antennas," in *Antennas: Theory and Practice*, chapter 10, pp. 321–322, John Wiley & Sons, New York, NY, USA, 1952.